Song *et al.*
Biotechnology for Biofuels and Bioproducts (2025) 18:29
https://doi.org/10.1186/s13068-025-02627-4

Biotechnology for Biofuels and Bioproducts

RESEARCH

Open Access

Transcriptome analysis and reverse engineering verification of SNZ3^{Val125Ile} and Pho3^{Asn134Asp} revealed the mechanism of adaptive laboratory evolution to increase the yield of tyrosol in *Saccharomyces cerevisiae* strain S26-AE2

Na Song[1], Huili Xia[2], Xiaoxue Yang[1], Siyao Liu[1], Linglong Xu[1], Kun Zhuang[1,3], Lan Yao[1], Shihui Yang[4], Xiong Chen[1*] and Jun Dai[1,4*]

Abstract

Background Tyrosol is an important drug precursor, and *Saccharomyces cerevisiae* is one of the main microorganisms that produces tyrosol. Although excessive metabolic modification increases the production of tyrosol, it also causes a decrease in the growth rate of yeast. Therefore, this study attempted to restore the growth of *S. cerevisiae* through adaptive evolution and further improve tyrosol production.

Results After the adaptive laboratory evolution of *S. cerevisiae* S26, three evolutionary strains were obtained. The biomass of strain S26-AE2 reached 17.82 g DCW/L in the presence of 100 g/L glucose, which was 15.33% higher than that of S26, and its tyrosol production reached 817.83 mg/L. The transcriptome analysis revealed that, upon exposure to 100 g/L glucose, the S26-AE2 strain may reduce the transcriptional regulation of glucose repression through decreased *HXK2* expression. The expression of genes related to pyruvate synthesis was increased in strain S26-AE2. Meanwhile, the expression levels of most tricarboxylic acid cycle-related genes in S26-AE2 were increased when cultured with 20 g/L glucose. Furthermore, the amount of tyrosol produced by strain S26 with the SNZ3^{Val125Ile} mutation increased by 17.01% compared with that of the control strain S26 following exposure to 100 g/L glucose.

Conclusions In this study, a strain, S26-AE2, with good growth and tyrosol production performance was obtained by adaptive evolution. The transcriptome analysis revealed that the differences in the expression of genes involved in metabolic pathways in adaptive evolutionary strains may be related to yeast growth and tyrosol production. Further reverse engineering verified that the mutation of *SNZ3* promoted tyrosol synthesis in *S. cerevisiae* in glucose-rich medium. This study provides a theoretical basis for the metabolic engineering of *S. cerevisiae* to synthesise tyrosol and its derivatives.

*Correspondence:
Xiong Chen
cx163_qx@163.com
Jun Dai
jundai@hbut.edu.cn
Full list of author information is available at the end of the article

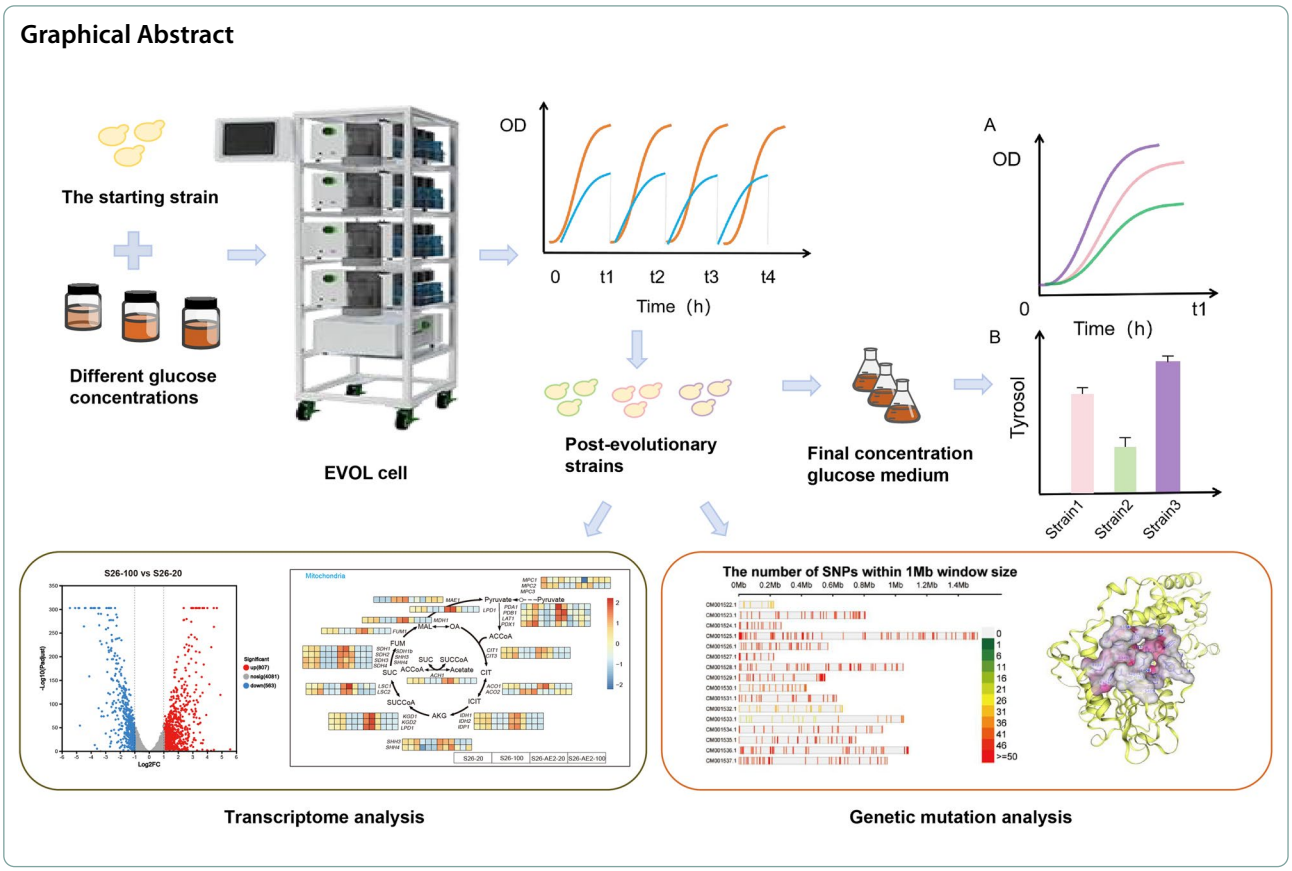

Background

Tyrosol is the precursor of salidroside and hydroxytyrosol and has various pharmaceutical activities, such as anticancer, antioxidant, and anti-inflammatory activities [1, 2]. It mainly exists in olive oil, wine, and plant tissues and is a phenethyl alcohol derivative. At present, the commercial production of tyrosol mainly depends on chemical synthesis and olive leaf extraction [3–5]. However, the olive leaf extraction method faces the problem of a low extraction efficiency, and its production is highly dependent on the supply of olive leaf resources. More importantly, both methods are not environmentally friendly, whether extraction or chemical synthesis. In contrast, microbial cell factories exhibit many characteristics that are conducive to the low-cost, environmentally friendly, and sustainable production of tyrosol [6]. In recent years, *Saccharomyces cerevisiae* and *E. coli* have been successfully used to produce tyrosol [7–10]. These studies revealed that the tyrosol concentration was 1.3 g/L in *S. cerevisiae* [11] and 2.12 g/L in *E. coli* [12]. Although a certain amount of high yield has been achieved in *S. cerevisiae*, with increasing modification, the robustness of the yeast is reduced. In previous work, a strain of *S. cerevisiae* S26 with a high yield of tyrosol was constructed. However, excessive modification decreases the vigorous growth of yeast, which greatly limits its application in fermentation tanks and industrial production.

Adaptive laboratory evolution (ALE) is an efficient method for obtaining strains with improved traits [13]. Through natural selection, many mutants accumulate to quickly obtain strains with ideal characteristics. ALE has been applied to optimise the growth rate of various industrial-related microbial species, to improve the growth defects of engineered strains, and to study how and why the growth rate changes during evolution [14]. ALE can also be combined with a bioinformatics analysis and reverse engineering to understand the basic mechanism of molecular evolution and the adaptive changes that accumulate in the long-term selection process of microbial populations under specific growth conditions. Zongjie Dai et al. combined rational design, adaptive laboratory evolution, and reverse engineering, and observed that the specific growth rate of the best strain reached 0.218 h^{-1}, which is close to the maximum growth rate of *S. cerevisiae* with purely respiratory metabolism [15]. Henri Ingelman et al. used three different and independent adaptive laboratory evolution strategies to evolve wild-type *Clostridium autoethanogenum* to grow faster

without yeast extract and to be robust in operating continuous bioreactor cultures [16]. Kuk-Ki Hong et al. improved the growth rate of *S. cerevisiae* under specific conditions of galactose supplementation by adaptive evolution [17]. Ryan A. LaCroix et al. used adaptive laboratory evolution and observed that key mutations caused *E. coli* K-12 MG1655 to grow rapidly on glucose-based media [18]. Eugen Pfeifer et al. performed a comparative adaptive laboratory evolution experiment on *Corynebacterium glutamicum* ATCC 13032 and its phage-free variant MB001, thereby increasing the growth rate on the medium with the lowest glucose concentration [19].

In this study, *S. cerevisiae* S26 was used as the starting strain for laboratory evolution [20]. Throughout the evolutionary process, the glucose concentration progressively increased. Three strains, S26-AE1, S26-AE2, and S26-AE3, were isolated during the evolutionary phase, and strain S26-AE2, which exhibited superior fermentation characteristics and a high yield of tyrosol, was selected for further investigation. The transcriptome analysis of the evolutionary strain S26-AE2 revealed changes in the expression of genes involved in the metabolic pathway of yeast after evolution. Increases in the activity of the TCA cycle and aromatic amino acid gene expression may affect the growth recovery of *S. cerevisiae* and increase the tyrosol content. The single-nucleotide polymorphism (SNP) mutations $PHO3^{Asn134Asp}$ and $SNZ3^{Val125Ile}$ were screened, and reverse engineering verification was performed. The results showed that the $SNZ3^{Val125Ile}$ mutation was positively correlated with tyrosol production in yeast. These results provide ideas for obtaining more robust industrial *S. cerevisiae* strains and a theoretical basis for further modification of the strain to increase tyrosol production.

Results

Adaptive laboratory evolution of *S. cerevisiae* S26 for improved growth phenotypes

Adaptive laboratory evolution was performed to improve the growth phenotype of *S. cerevisiae* S26. The initial medium was YEPD, and during the evolutionary process, the glucose concentration in the YEPD medium progressively increased. As shown in Fig. 1, the evolutionary process underwent three stages. In stage 1, the glucose concentration was increased to 40 g/L, and the strain was named S26-AE1. At this stage, the average passage time was 16 h. In stage 2, the glucose concentration was increased from 40 to 80 g/L. A total of 20 passages were conducted in this stage, and strain S26-AE2 was obtained. The strain was passaged once every 11.75 h on average, and was shorter than stage 1. In stage 3, the glucose content increased from 80 to 125 g/L, and the strain was passaged once every 11.95 h on average. The evolutionary strain in stage 3 was named S26-AE3.

The cellular morphology of the yeast was subsequently observed by scanning electron microscopy (SEM) (Fig. 2A). A small amount of cell damage was observed in S26-AE1. S26-AE2 showed obvious cell damage, which may be attributed to the premature transition of cells into the stable phase or an increase in the sugar concentration. However, with a further increase in the evolutionary sugar concentration, the S26-AE3 strain did not exhibit more cell damage. We performed spot assays of strains S26-AE1, S26-AE2, and S26-AE3 in the presence of 20 g/L and 100 g/L glucose to investigate the growth phenotypes of the strains after ALE (Fig. 2B). The growth of the evolutionary strains in media containing 20 g/L and 100 g/L glucose

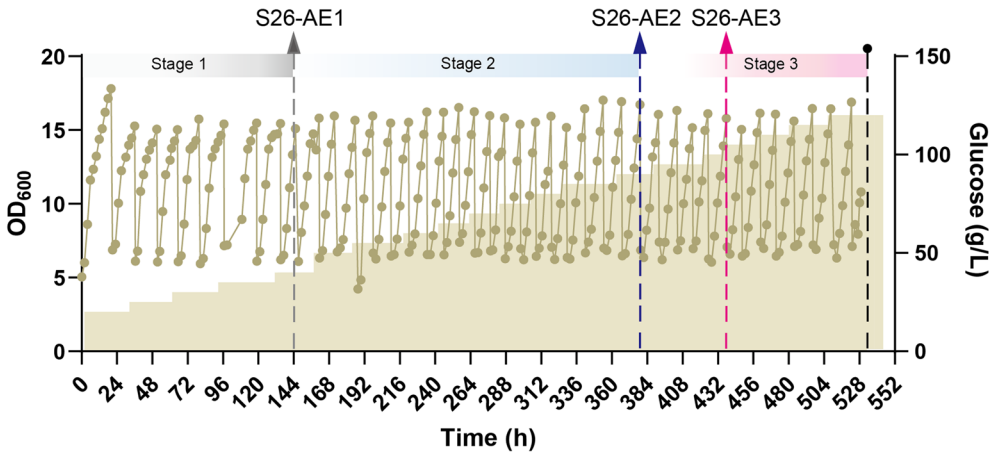

Fig. 1 Diagram showing the adaptive laboratory evolution of *S. cerevisiae* strain S26. The total evolution time was 529 h, and the evolution process was divided into three stages

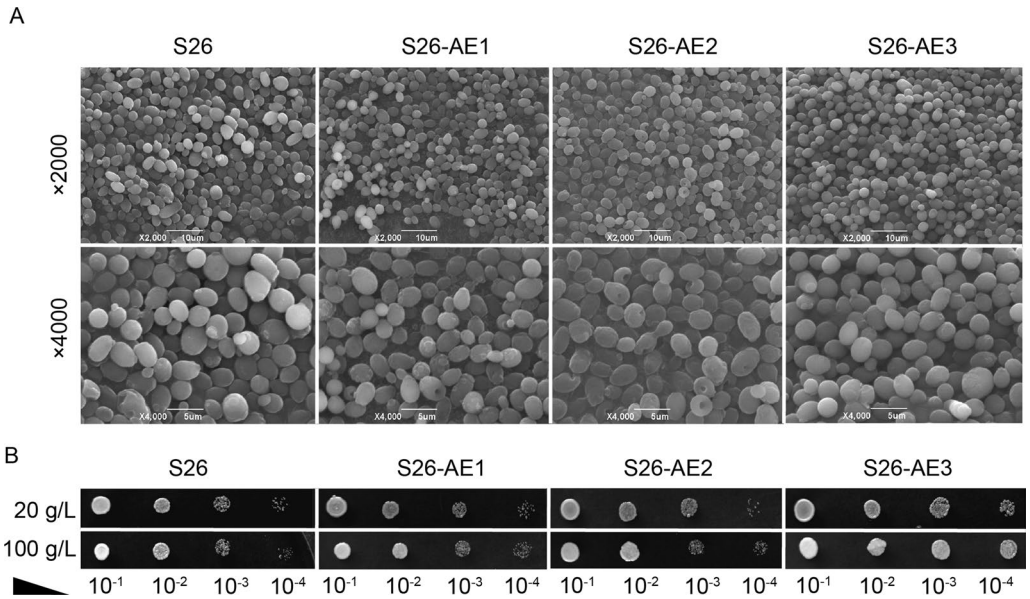

Fig. 2 **A** The cellular morphology of the original strain and the evolved strains cultured in 100 g/L glucose medium for 24 h was observed by scanning electron microscopy. **B** Picture of the spot assay. After the original strain and the evolved strain were cultured on solid YEPD medium containing 20 g/L or 100 g/L glucose, for 24 h, images were captured

was better than that of the original strain, indicating that adaptive laboratory evolution was conducive to improving strain growth.

Changes in the fermentation performance of evolutionary strains

The starting strain S26 and the evolutionary strains S26-AE1, S26-AE2, and S26-AE3 were cultured in YEPD medium supplemented with 100 g/L glucose to determine the fermentation performance of evolutionary strains. As shown in Fig. 3A, the starting strain S26 entered the stationary phase within 48 h, with an average OD_{600} of 36.39 and a dry weight of 15.45 g DCW/L. The biomass of S26-AE1 was 8.99% higher than that of S26 at 48 h (Fig. 3B). S26-AE2 entered a stable phase after 24 h, which was earlier than that of strain S26 (Fig. 3C). The OD_{600} during this period was 38.45, and the biomass of strain S26-AE2 was 17.82 g DCW/L at 48 h, which was 15.33% higher than that of strain S26. Similarly, strain S26-AE3 also entered the stationary phase after 24 h, with an OD_{600} of 39.14 (Fig. 3D). The reason why S26-AE2 and S26-AE3 entered the stationary phase earlier than the original strain may be an adaptation to the 100 g/L glucose environment and their rapid utilisation of glucose.

We further detected the tyrosol content to explore whether the adaptation of yeast to a high-glucose environment was helpful for enhancing the de novo synthesis of tyrosol. As shown in Fig. 3F, the maximal tyrosol production of S26 was 483.35 mg/L at 60 h, which was somewhat lower than that on the YEPD medium (538.41 mg/L) [20]. However, tyrosol production was not significantly different between strains S26-AE1 and S26. Surprisingly, the tyrosol production of S26-AE2 improved significantly, especially at 48 h, and its tyrosol production reached 817.83 mg/L, which was 69.20% higher than the highest yield of strain S26-AE1. However, tyrosol production in strain S26-AE3 reached 553.79 mg/L after 72 h of fermentation (Fig. 3H). The evolution of S26-AE2 was beneficial for the production of tyrosol.

We further explored the growth characteristics and physiological characteristics of the evolved strains by determining the indicators of glucose consumption and the production of ethanol, glycerol, and trehalose. The glucose consumption and ethanol production of the starting strain and the evolutionary strain were compared. The residual glucose concentration of the starting strain S26 in fermentation medium after 12 h was 89.30 g/L, and the glucose concentration of the evolutionary strain S26-AE1 was 38.05 g/L. At this time, the ethanol production was 4.20 g/L and 23.08 g/L, respectively (Fig. 4A, B). The evolved strains S26-AE2 and S26-AE3 completely consumed glucose after 12 h and produced 34.16 g/L and 36.12 g/L ethanol, respectively (Fig. 4C, D).

In addition, strains S26 and S26-AE1 accumulated a certain amount of trehalose in the extracellular space during fermentation (Fig. 4E, F). Compared with that of the other strains, the trehalose production of strains

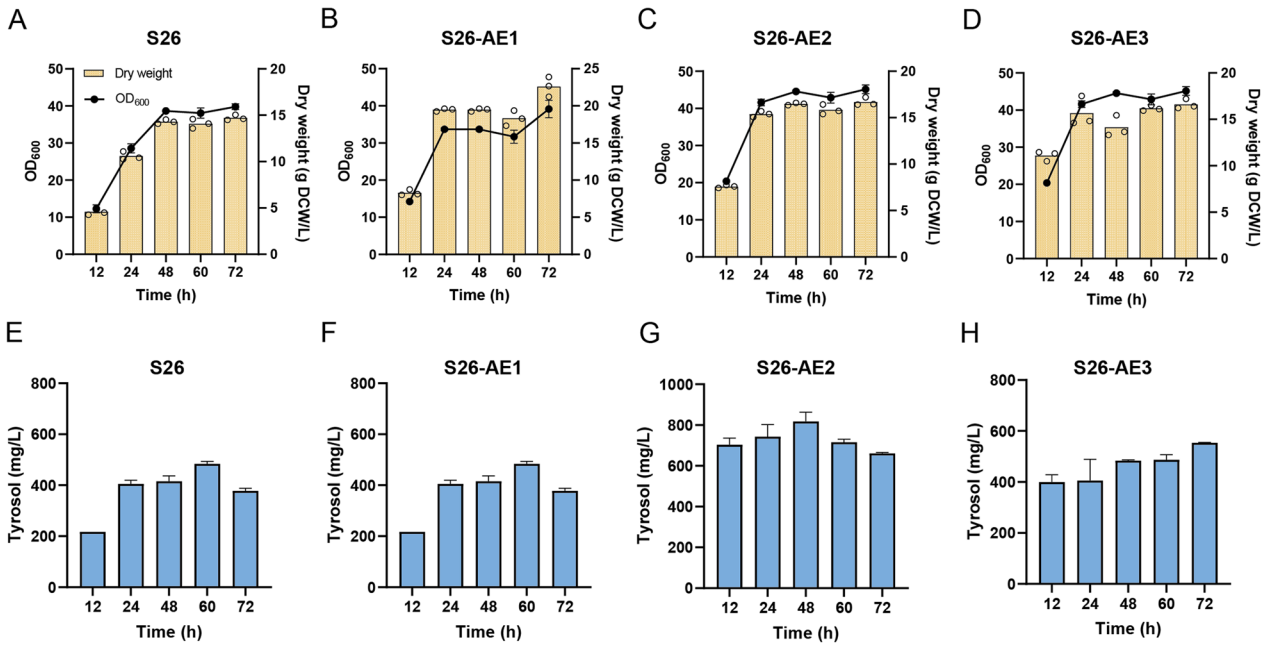

Fig. 3 **A**, **B**, **C**, and **D** The OD_{600} and dry weight of strains S26, S26-AE1, S26-AE2, and S26-AE3, which were cultured in YEPD liquid medium supplemented with 100 g/L glucose. **E**, **F**, **G**, and **H** Tyrosol production by strains S26, S26-AE1, S26-AE2, and S26-AE3, which were cultured in YEPD liquid medium supplemented with 100 g/L glucose

S26-AE2 and S26-AE3 was significantly reduced (Fig. 4G, H). The intracellular glycerol content of strain S26 was 0.0378 mM at 24 h of fermentation, and the glycerol contents of strains S26-AE1, S26-AE2, and S26-AE3 were 0.0103 mM, 0.0243 mM, and 0.0083 mM, respectively (Fig. 4I, J, K, L). Both trehalose and glycerol play a role in preserving the osmotic pressure in cells, thereby reducing the damage caused by external stress to cells. In the process of evolution, the strains reduced the production of trehalose and glycerol, suggesting that the evolved strains gradually adapted to grow on 100 g/L glucose medium.

Transcriptome analysis of the mechanisms underlying adaptive evolution leading to increased tyrosol production in strain S26-AE2

We explored the mechanism of the increases in the S26-AE2 biomass and tyrosol production after evolution by performing a transcriptome analysis of the changes in gene expression in strains S26 and S26-AE2. The strains were cultured with 20 g/L glucose or 100 g/L glucose, and RNA was extracted for the transcriptome determination after 24 h of culture. According to the transcriptome results, the genes whose expression differed significantly are shown in volcano plots in Fig. 5. S26 had 807 upregulated genes and 583 downregulated genes in the presence of 100 g/L glucose compared with 20 g/L glucose (Fig. 5A). Compared with S26, S26-AE2 presented 36 upregulated genes and 1 downregulated gene in the presence of 20 g/L glucose (Fig. 5B). Compared with S26-AE2 cultured with 20 g/L glucose, S26-AE2 cultured with 100 g/L glucose presented 779 upregulated genes and 621 downregulated genes (Fig. 5C). Compared with the original strain S26, the evolutionary strain S26-AE2 had 9 upregulated genes and 16 downregulated genes in the presence of 100 g/L glucose (Fig. 5D). This result indicated that the metabolism of the strains differed significantly after laboratory evolution, and these differences may be due to the recovery of growth or the improvement in tyrosol production.

We further studied the roles of these differentially expressed genes in metabolic pathways by mapping them to metabolic pathways. As shown in Fig. 6A, *HXT5* is a low/medium-affinity glucose transporter gene, and the expression of the *HXT5* gene increased significantly in strain S26-AE2 in the presence of 20 g/L glucose. Stefan Buziol et al. reported that the *HXT5* gene was not expressed during the growth of yeast cells in rich media supplemented with glucose or raffinose. However, it was strongly induced during nitrogen or carbon starvation [21]. The expression levels of *HXK1* and *GLK1* were lower under 100 g/L glucose conditions than under 20 g/L glucose conditions in both strains S26 and S26AE-2, which is similar to the findings of previous studies (Fig. 6A) [22]. In strain S26, the expression of *HXK2* under 100 g/L glucose conditions was significantly higher than that under 20 g/L glucose conditions and higher than the expression

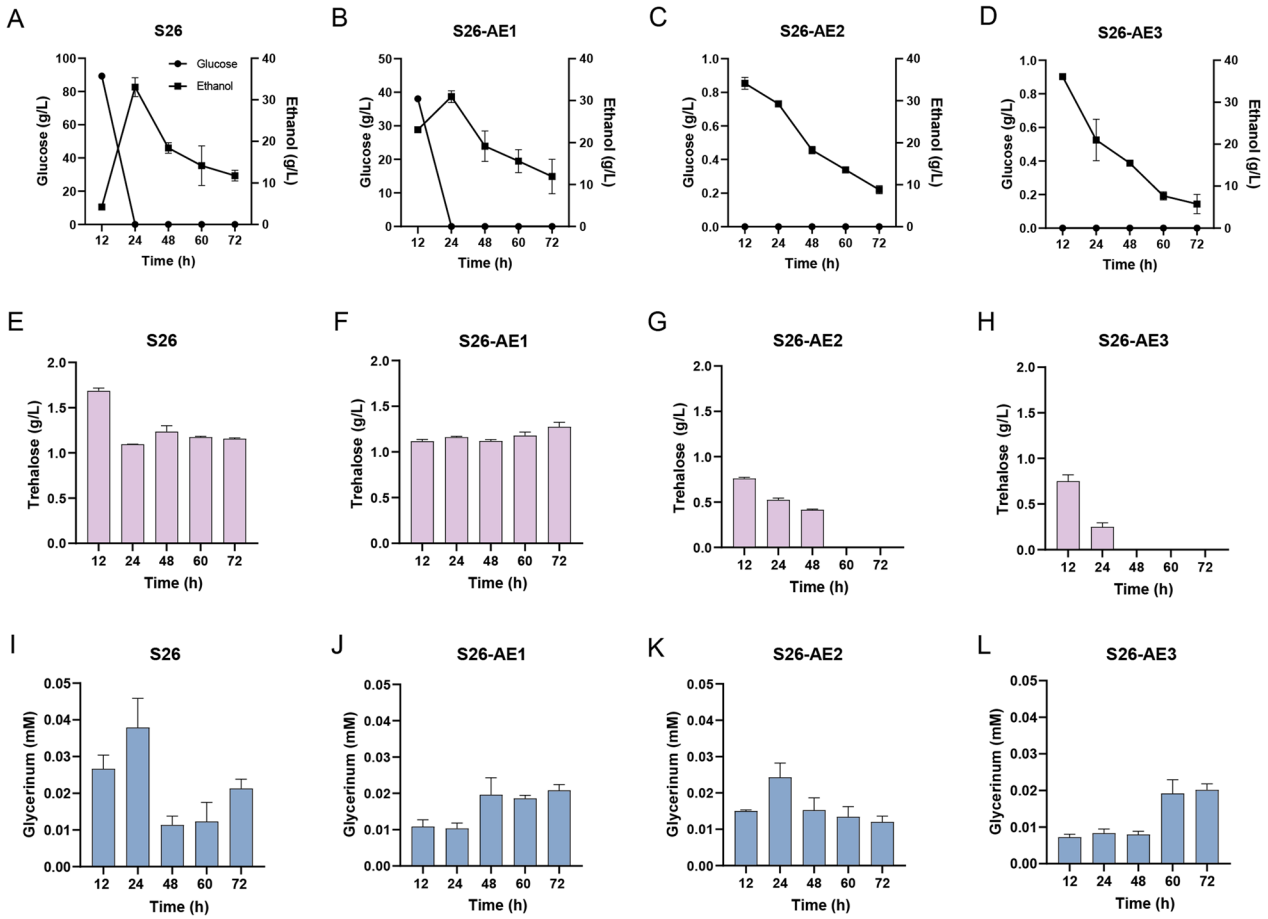

Fig. 4 **A**, **B**, **C**, and **D** Glucose consumption and ethanol production by strains S26, S26-AE1, S26-AE2, and S26-AE3, which were cultured in YEPD liquid medium supplemented with 100 g/L glucose. **E**, **F**, **G**, and **H** Changes in the trehalose contents in strains S26, S26-AE1, S26-AE2, and S26-AE3, which were cultured in YEPD liquid medium supplemented with 100 g/L glucose. **I**, **J**, **K**, and **L** Changes in the glycerol contents of strains S26, S26-AE1, S26-AE2, and S26-AE3, which were cultured in YEPD liquid medium containing 100 g/L glucose

of *HXK2* in strain S26AE-2. According to Rodríguez A et al. when glucose is present in the culture medium, the *GLK1* gene is either not expressed or expressed at a very low level, and the transcription of the *HXK1* and *GLK1* genes is automatically regulated by glycolytic products and themselves [23]. *HXK2* is a dual-function hexokinase that acts as a glycolytic enzyme and is involved in the transcriptional regulation of glucose-responsive genes [24]. *HXK2* also plays an important regulatory role in glucose repression [25–27]. According to these studies, we speculated that after adaptive evolution, the decreased expression of *HXK2* in strain S26-AE2 reduced the transcriptional regulation of glucose repression in cells.

PGI1 (phosphoglucose isomerase 1) catalyses the interconversion of glucose 6-phosphate and fructose 6-phosphate, and glucose 6-phosphate is entirely rerouted into the PP pathway. The expression of the *PGI1* gene in strain S26-AE2 increased slightly under 100 g/L glucose conditions (Fig. 6A). Related research has shown that *PGI1* deletion mutants of *S. cerevisiae* cannot grow on glucose as the sole carbon source and are even inhibited by glucose [28]. Therefore, the increase in *PGI1* gene expression may promote the utilisation of glucose by the evolutionary strain S26-AE2, which was consistent with the increase in the glucose consumption rate (Fig. 4C).

In the presence of 100 g/L glucose, the expression of the *GPD1*, *GPD2*, and *GPP2* genes increased in both S26 and S26-AE2 (Fig. 6A). The *GPD1* gene, an osmotic induction-related gene, encodes glycerol-3-phosphate dehydrogenase, and the expression of *GPD1* is the result of the interplay between different signalling pathways [29]. The deletion of structural genes such as *GPD1* and *GPD2* leads to osmosensitivity in yeast, which is not desirable for industrial strains [30, 31]. *GPP1* is an isoenzyme that catalyses the formation of glycerol and is also involved in the formation of acetic acid. In the previous work, *GPP1* was knocked out to reduce the production of acetic acid by the heterologous phosphoketolase

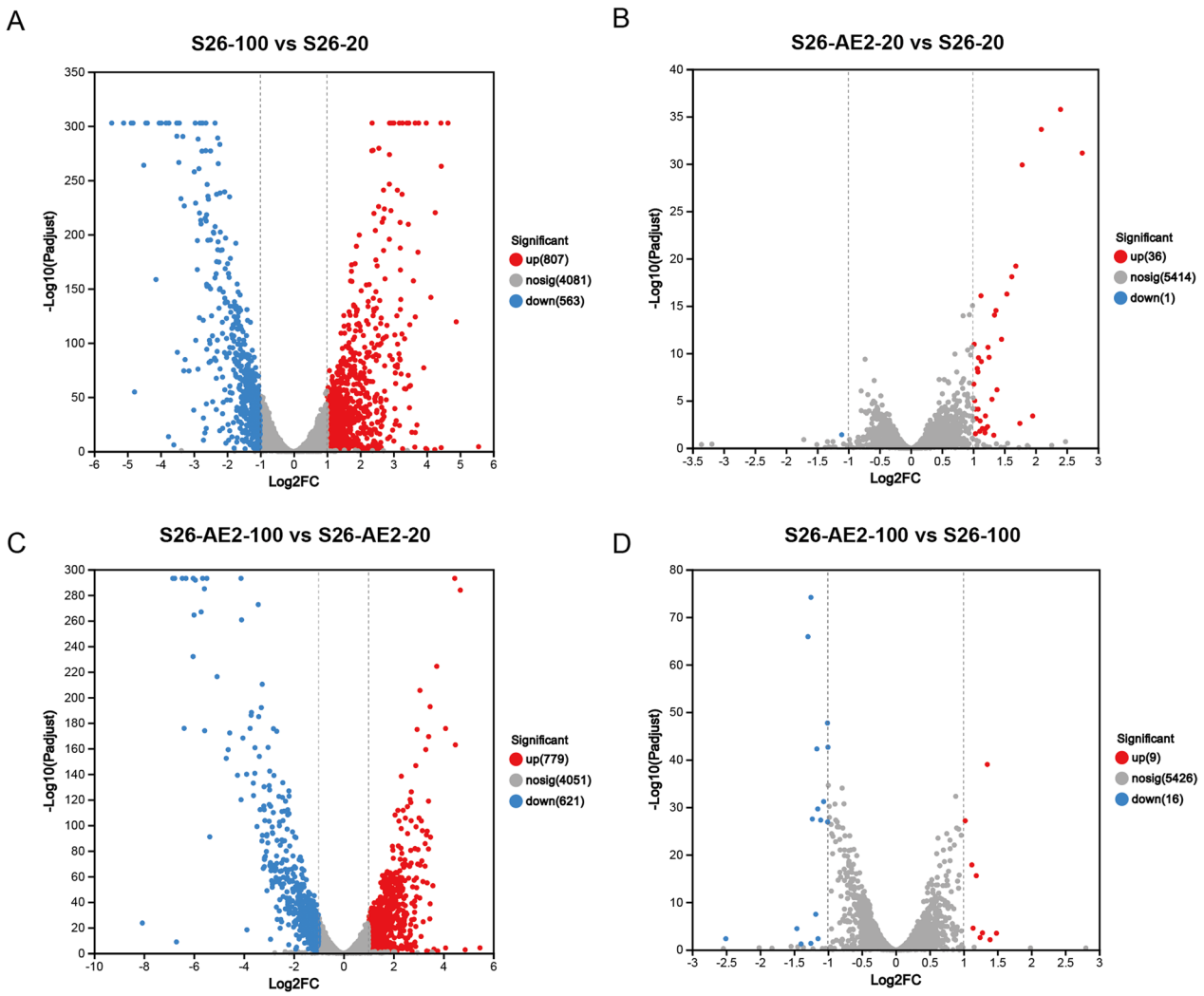

Fig. 5 Volcano plots showing the gene expression levels in strains S26 and S26-AE2 cultured with 20 g/L or 100 g/L glucose. **A** The number of differentially expressed genes in group S26-100 compared with group S26-20. **B** The number of differentially expressed genes in group S26-AE2-20 compared with group S26-20. **C** The number of differentially expressed genes in group S26-AE2-100 compared with group S26-AE2-20. **D** The number of differentially expressed genes in group S26-AE2-100 compared with group S26-100. Group S26-20 represents strain S26 cultured under 20 g/L glucose conditions, and group S26-100 represents strain S26 cultured under 100 g/L glucose conditions. Group S26-AE2-20 represents strain S26-AE2 cultured under 20 g/L glucose conditions, and group S26-AE2-100 represents strain S26-AE2 cultured under 100 g/L glucose conditions

(PHK) pathway [20]. However, due to the presence of *GPP2*, the knockout of *GPP1* does not seem to affect glycerol production. The expression of the *GPP2* gene in S26-AE2 was slightly lower than that in S26, which was consistent with the results of the glycerol determination (Fig. 4K). Glycerol enters the glycolytic pathway through the sequential actions of two genes, namely, the cytosolic glycerol kinase GUT1 and the glycerol-3-phosphate dehydrogenase GUT2 [32]. Interestingly, the expression of *GUT2* in strain S26-AE2 increased upon stimulation with 20 g/L glucose.

Pyruvate, a precursor for several amino acids, can be synthesised from phosphoenolpyruvate by pyruvate kinase [33]. The gene expression levels of *PGK1*, *GPM1*, *GPM2*, *ENO1*/*ENO2*, and *PYK1*, which are involved in pyruvate production, in strain S26-AE2 were higher than those in strain S26 (Fig. 6A). Therefore, the evolved strain S26-AE2 is likely to increase the production of pyruvate. In addition, the expression of *PYK2* was low in the presence of 100 g/L glucose. Related studies have shown that the absence of *PYK2* has no effect on the specific growth rate when glucose is used as a carbon source, which may

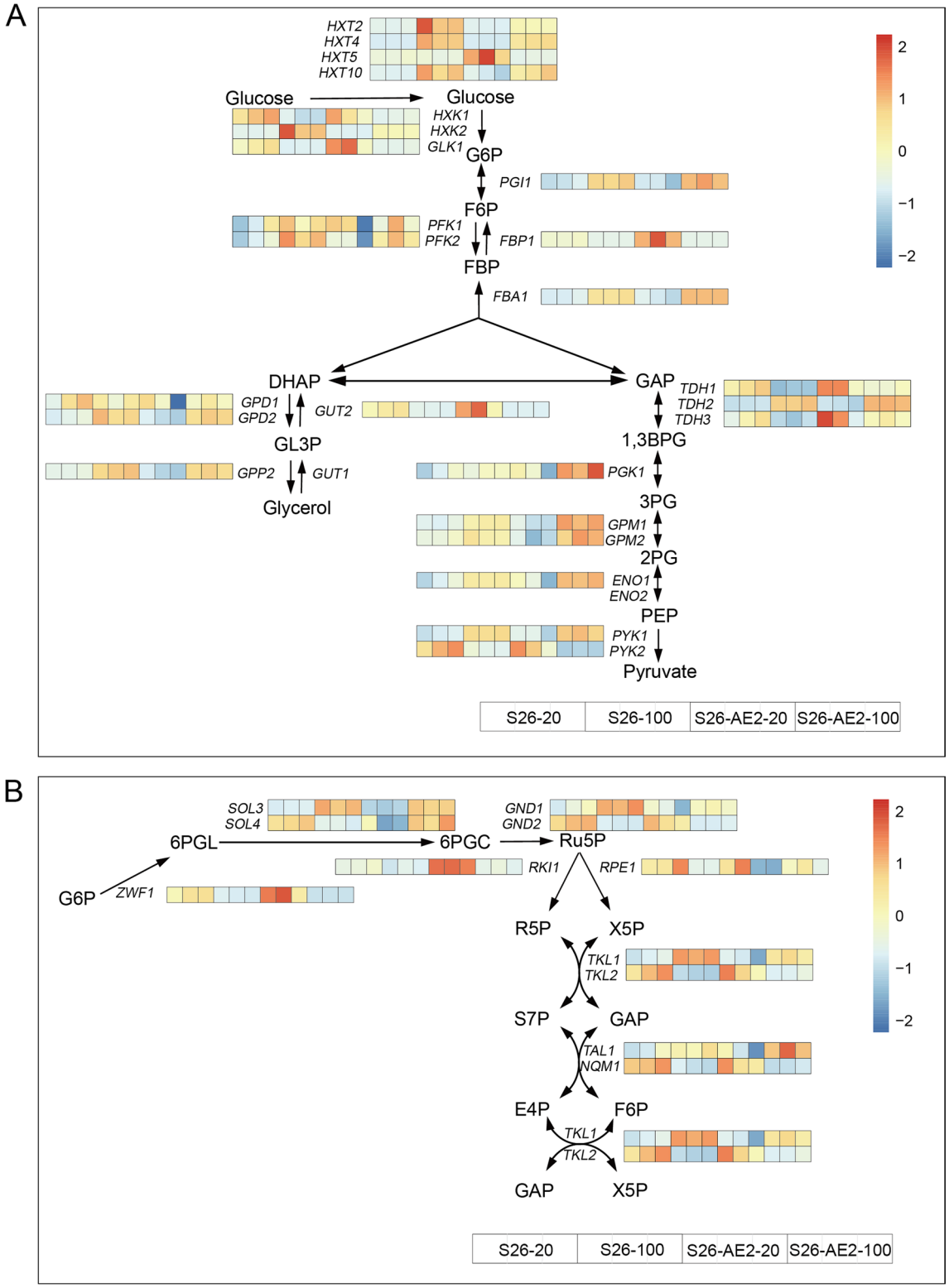

Fig. 6 Map of the metabolic pathways related to the differentially expressed genes in strains S26 and S26-AE2 under 20 g/L and 100 g/L glucose conditions. **A** Glycolysis pathway. **B** The pentose phosphate pathway. **C** Tricarboxylic acid (TCA) cycle. **D** Glyoxylic acid pathway. **E** The tyrosol synthesis pathway

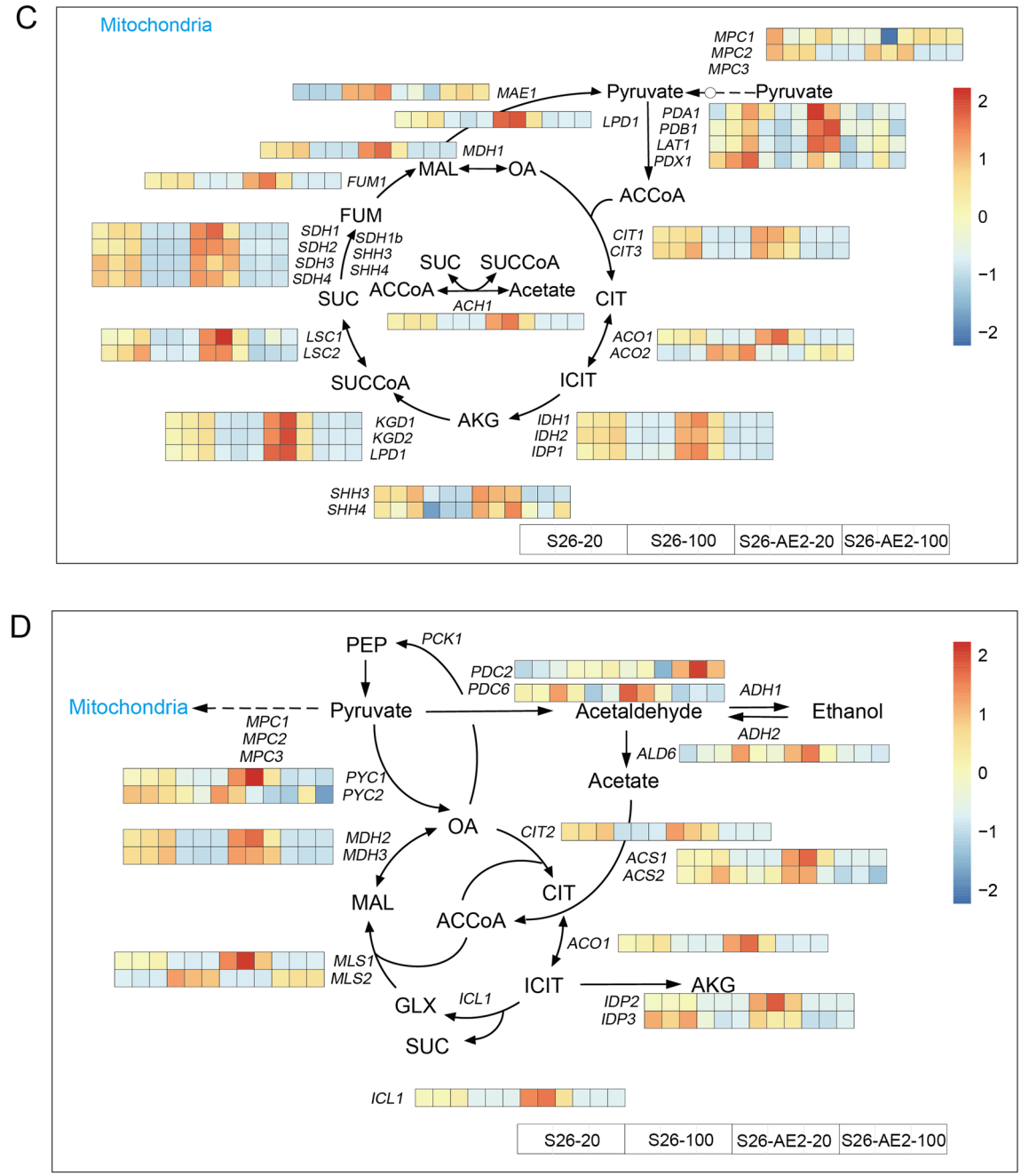

Fig. 6 continued

also explain why the expression of *PYK2* is low under 100 g/L glucose conditions [33].

The pentose phosphate pathway (PPP) is a mechanism of the oxidative decomposition of glucose. In the presence of 20 g/L glucose, the expression of the *SOL*3, *GND*1, and *TKL*1 genes was downregulated in strain S26, and the expression of the *SOL*4, *GND*2, and *TKL*2 genes was upregulated, similar to the findings of Bergman A et al. (Fig. 6B) [34]. Under 100 g/L glucose conditions, the expression pattern of the *SOL*3/4, *GND*1/2, and *TKL*1/2 genes was opposite that under 20 g/L glucose conditions. However, after evolution, these phenomena were not very obvious in strain S26-AE2. *SOL3* and *SOL4* expression was downregulated in strain S26-AE2 under 20 g/L glucose conditions and upregulated under 100 g/L glucose conditions. In addition, under the condition of

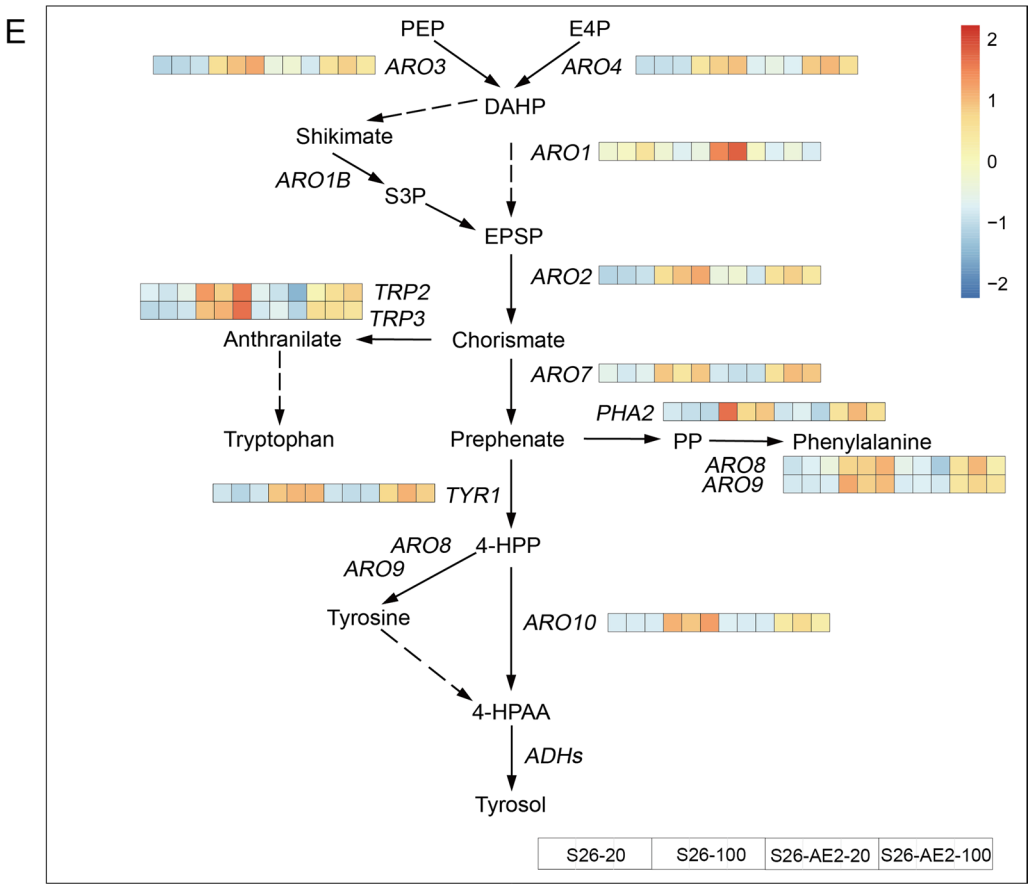

Fig. 6 continued

20 g/L glucose, the expression levels of *ZWF1* and *RKI1* increased in strain S26-AE2 (Fig. 6B), and were significantly higher than those in strain S26, whereas the expression levels of these genes were downregulated under the condition of 100 g/L glucose, indicating that the genes were regulated by the external glucose content. *ZWF1* is an $NADP^+$-dependent dehydrogenase, and the overexpression of *ZWF1* can increase the supply of NADPH in yeast cells [35].

The TCA cycle is an important hub of energy metabolism. The transcriptome analysis showed that most of the genes involved in the TCA cycle were upregulated under 20 g/L glucose conditions and that gene expression was downregulated under 100 g/L glucose conditions (Fig. 6C). In addition, gene expression in strain S26-AE2 under 20 g/L glucose conditions was clearly significantly higher than that in strain S26. These findings indicated that the TCA cycle-related genes of the evolutionary strains were more active. The genes with relatively high expression levels included the SDH (succinate dehydrogenase) enzyme family, the LSC (succinyl-CoA ligase) enzyme, and the KGO enzyme. However, the difference was not obvious in the presence of 100 g/L glucose, suggesting that this difference may be related to the extracellular glucose content (Fig. 6C). An increase in TCA cycle activity promotes the consumption of pyruvate, which is derived mainly from the decomposition of glucose by cells. The TCA cycle promotes cell growth and energy generation, which in a certain sense explains the recovery of strain growth through glucose evolution. In the presence of 100 g/L glucose, the expression levels of the *MPC1*, *PDB1*, *LAT1*, *PDX1*, *SHH4*, and *LSC1* genes in the evolutionary strains were slightly higher than those in strain 26, and the expression levels of *ACO2* and *MAE1* decreased. Mitochondrial pyruvate carrier (MPC) complexes are responsible for the uptake of cytoplasmic pyruvate into mitochondria and are dissimilated by the pyruvate dehydrogenase complex and the oxidative TCA cycle; these complexes are used to generate energy or as precursors for the biosynthesis of branched-chain amino acids [36]. Therefore, the increased expression of the *MPC1* gene in the evolutionary strain under 100 g/L glucose conditions might increase the intake of

pyruvate and reduce the accumulation of pyruvate produced by glycolysis.

The glyoxylic acid cycle is particularly important for plants and some microorganisms. This pathway is the compensatory pathway of the TCA cycle. Through the glyoxylic acid cycle, yeast can use fatty acids and acetic acid as the sole carbon sources to synthesise carbohydrates, amino acids, and proteins to maintain normal cell growth. In the presence of 20 g/L glucose, the expression levels of the *PYC1*, *MDH2*, *MDH3*, *MLS1*, *IDP2*, *ACS1*, *ACS2*, *ALD6,* and *PDC6* genes in the evolutionary strain were significantly higher than those in the original strain (Fig. 6D). *ACS1* and *ACS2* are involved in acetic acid consumption. *PCK1* catalyses the conversion of oxaloacetate (OA) to phosphoenolpyruvate (PEP), and *PYC1* catalyses the conversion of pyruvate to OA. These two reactions are important steps in the gluconeogenesis pathway and are required to consume nonglucose carbon sources (such as ethanol or acetate) (Fig. 6D). During the construction of our previous strain, *PDC1* was knocked out, and the expression of *PDC2* increased after adaptive evolution [20]. This phenomenon shows that the metabolic capacity of evolved yeast has increased, but is not conducive to the production of tyrosol.

The expression levels of *ARO3* and *ARO4* under 100 g/L glucose conditions were higher than those under 20 g/L glucose conditions (Fig. 6E). The increased expression of *ARO3* and *ARO4* promotes the formation of DAHP and increases tyrosol production, which also explains the increase in the tyrosol content in strain S26-AE2. Similarly, the increased expression of *ARO2*, *ARO7*, *TYR1,* and *ARO10* promoted the synthesis of tyrosol. The results showed that the appropriate concentration of glucose could mobilise aromatic amino acid synthesis.

SNP mutation analysis of the adaptive laboratory evolutionary strain S26-AE2

We performed gene sequencing on the evolutionary strain S26-AE2 to obtain SNP-related information and identify changes related to growth and tyrosol production at the genetic level. Aligning all the SNPs to chromosomes revealed that SNPs mainly occurred in CM001525.1 and CM001529.1 (Fig. 7A). The number of SNPs that occurred on all introns was subsequently statistically analysed to obtain a petal diagram (Fig. 7B), which represents the number of SNP-containing genes after a comparison between the two groups. The results revealed 19 SNP mutations in S26-AE2-100vsS26-20, S26-AE2-100vsS26-AE2-20, and S26-100vsS26-20. Next, 19 SNPs were screened and analysed to obtain the data presented in Table 1. The results revealed five genes with SNP mutations, namely, *MAL32*, *SNZ3*, *DOT6*, *HXT3,* and *PHO3*.

MAL32 encodes alpha-glucosidase, which is involved in carbohydrate transport and metabolism. The deletion of *MAL31* and *MAL32* may have led to the aneuploidy of CHRIII, which harbours the *MAL2* locus [37]. SNZ3 is a subunit of pyridoxal 5'-phosphate synthase and a member of a stationary phase-induced gene family. The transcription of *SNZ3* is induced prior to a diauxic shift and in the absence of thiamine in a Thi2p-dependent manner; *SNZ3* forms a coregulated gene pair with *SNO3* [38]. DOT6 is a transcriptional regulatory protein and is involved in rRNA and ribosome biogenesis. HXT3 is a low-affinity glucose transporter of the major facilitator superfamily, and its expression is induced under low- or high-glucose conditions. HXT3 has a paralogue, HXT5, that arose from whole-genome duplication. PHO3 is a constitutively expressed acid phosphatase similar to

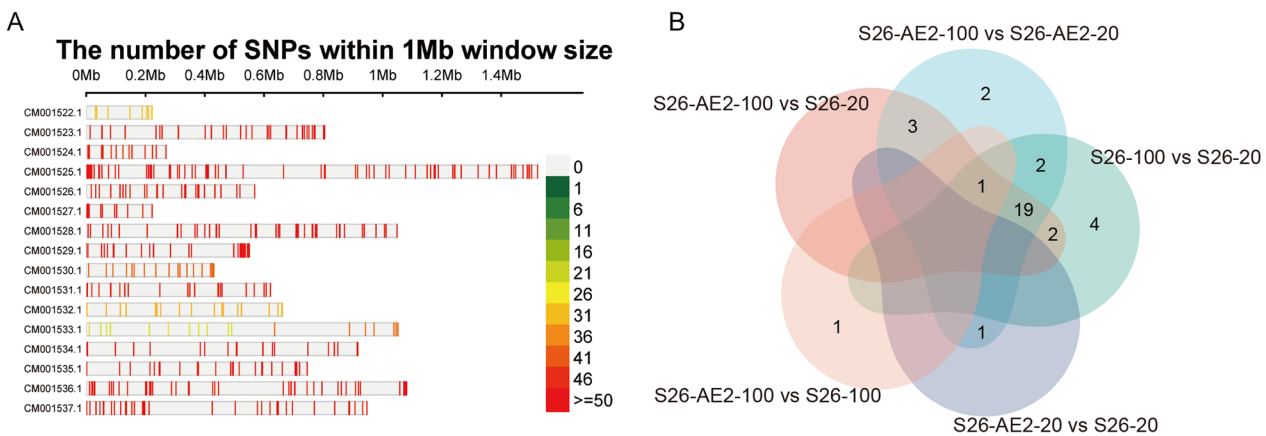

Fig. 7 **A** SNP density map of strain S26AE-2 showing the distribution of SNPs across chromosomes. **B** Petal map of SNP events representing the statistical analysis of SNPs in introns of groups S26-AE2-100vsS26-20, S26-AE2-100vsS26-100, S26-AE2-20vsS26-20, S26-100vsS26-20, and S26-AE2-100vsS26-AE2-20

Table 1 Proteins with SNP mutations contained in strain S26-AE2

Gene description	Chrom	Genome position	Ref	Alt	Anno	Gene description	Type	Mutations
MAL32	CM001523.1	800665	T	C	Exonic	Synonymous SNV	SNP	Phe472Phe
MAL32	CM001523.1	800863	G	A	Exonic	Synonymous SNV	SNP	Leu538Leu
SNZ3	CM001527.1	8368	C	T	Exonic	Synonymous SNV	SNP	Gly93Gly
SNZ3	CM001527.1	8416	C	T	Exonic	Synonymous SNV	SNP	Ile109Ile
SNZ3	CM001527.1	8443	C	T	Exonic	Synonymous SNV	SNP	Asn118Asn
SNZ3	CM001527.1	8455	A	G	Exonic	Synonymous SNV	SNP	Leu122Leu
SNZ3	CM001527.1	8462	G	A	Exonic	Nonsynonymous SNV	SNP	Val125Ile
DOT6	CM001526.1	332037	T	G	Exonic	Nonsynonymous SNV	SNP	Lys355Asn
DOT6	CM001526.1	332040	C	A	Exonic	Nonsynonymous SNV	SNP	Arg354Ser
HXT3	CM001525.1	1161695	A	C	Exonic	Synonymous SNV	SNP	Val538Val
PHO3	CM001523.1	422454	T	C	Exonic	Nonsynonymous SNV	SNP	Asn134Asp
PHO3	CM001523.1	422458	T	C	Exonic	Synonymous SNV	SNP	Ser132Ser
PHO3	CM001523.1	421594	A	G	Exonic	Synonymous SNV	SNP	Asp420Asp

1. "Chrom" means chromosome. 2. "Ref" means Reference sequence. 3. "Alt" means Alternative sequence. 4. "Anno" means Annotation

PHO5 that is transported to the cell surface via vesicles. It can hydrolyse thiamine phosphates in the periplasmic space and increase cellular thiamine uptake. The expression of *PHO3* is repressed by thiamine.

As shown in Table 1, SNZ3 contained mutations at amino acid residues 118, 122, and 125; synonymous mutations were identified at amino acids 118 and 122, and a nonsynonymous mutation was identified at amino acid residues 125. PHO3 was mutated at residues 132, 134, and 420, and only amino acid residues 420 exhibited a nonsynonymous mutation. DOT6 also had nonsynonymous mutations at residues sites 335 and 354. Next, we analysed the mutations in *SNZ3* and *PHO3*.

Molecular docking analysis of the SNZ3 and PHO3 mutants binding to small molecules

We simulated the catalytic pockets of the proteins before and after mutation and docked the original and mutated proteins with small molecules to compare the potential effects of *PHO3* and *SNZ3* mutations on the catalysis of the substrates thiamine phosphate and D-ribose 5-phosphate and the formation of thiamine and pyridoxine. The docking results showed that after the introduction of the $PHO3^{Asn134Asp}$ mutation, its Vina score for the interaction with the small-molecule substance thiamine phosphate decreased to −6.6, which indicated that the affinity between the receptor and the ligand improved (Table S3). Moreover, the interaction of the PRO51, PRO363, MET365, and GLY366 residues with small molecules was reduced, and the binding of the ALA348, ILE398, and CYS408 residues was increased (Fig. 8E and Table S4). After the PHO3 mutation, its Vina score decreased to -5.4 after docking with the small-molecule thiamine (Table S3). The binding of the THR81, ASP231, THR258, PHE260, SER288, TYR289, and VAL375 residues to the small-molecule thiamine was reduced, and the binding of the SER253 and LYS254 residues was increased (Fig. 8F and Table S4). After SNZ3 mutation, the Vina score for the interaction with the small-molecule D-ribose 5-phosphate decreased to −5.7 (Table S3), but the residues before and after mutation did not change (Fig. 8K and Table S4). After SNZ3 mutation, its Vina score for the interaction with pyridoxal was still −5.6, but the binding of the THR4 and ALA69 residues increased (Fig. 8L).

Reverse engineering verification improves yeast growth and robustness

We performed reverse engineering verification based on the screened mutation information to determine the functions of these mutant genes and their effects on yeast. Using CRISPR-Cas9 site-directed mutagenesis technology, we obtained three mutant strains, S26-$PHO3^{Mut}$, S26-$SNZ3^{Mut}$, and S26-$PHO3^{Mut}$ + $SNZ3^{Mut}$, with strain S26. The strains were cultured in YEPD medium supplemented with 20 g/L or 100 g/L glucose. The growth index and tyrosol production were measured after 72 h of culture. Under 20 g/L culture conditions, the tyrosol yield of the mutant strain S26-$SNZ3^{Mut}$ increased by 5.61% compared with that of the control strain S26 at 60 h (Fig. 9A, C). Under 100 g/L glucose culture, tyrosol production by the SNZ3 mutant increased by 17.01% compared with that of the control strain S26 at 72 h (Fig. 9E, E). The results showed that the mutation of SNZ3 promoted tyrosol production in yeast in 100 g/L glucose medium. Under 100 g/L culture conditions, the tyrosol production of the SNZ3 and PHO3 comutants increased by 11.37% compared with that of the control strain S26 at 72 h. Studies have shown that pyridoxine can promote

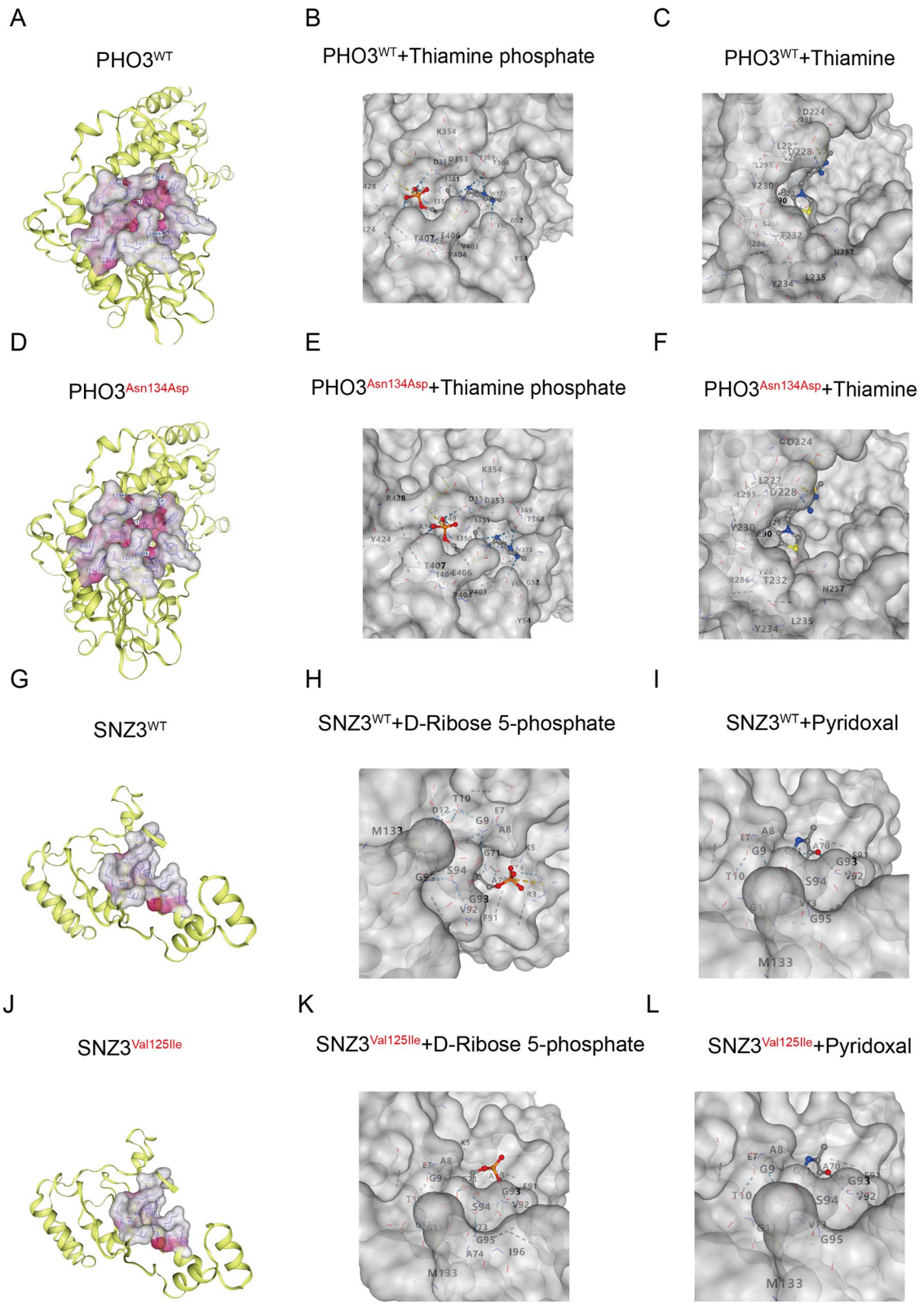

Fig. 8 **A**, **D**, **G**, and **J** Catalytic centres of the PHO3 and SNZ3 proteins before and after mutation. **B** and **C** Molecular docking of $PHO3^{WT}$ with thiamine phosphate and thiamine, respectively. **E** and **F** Molecular docking of $PHO3^{Asn134Asp}$ with thiamine phosphate and thiamine, respectively. **H**, **I** Molecular docking of SNZ^{WT} with D-ribose 5-phosphate and pyridoxal. **K** and **L** Molecular docking of $SNZ^{Val125Ile}$ with D-ribose 5-phosphate and pyridoxal

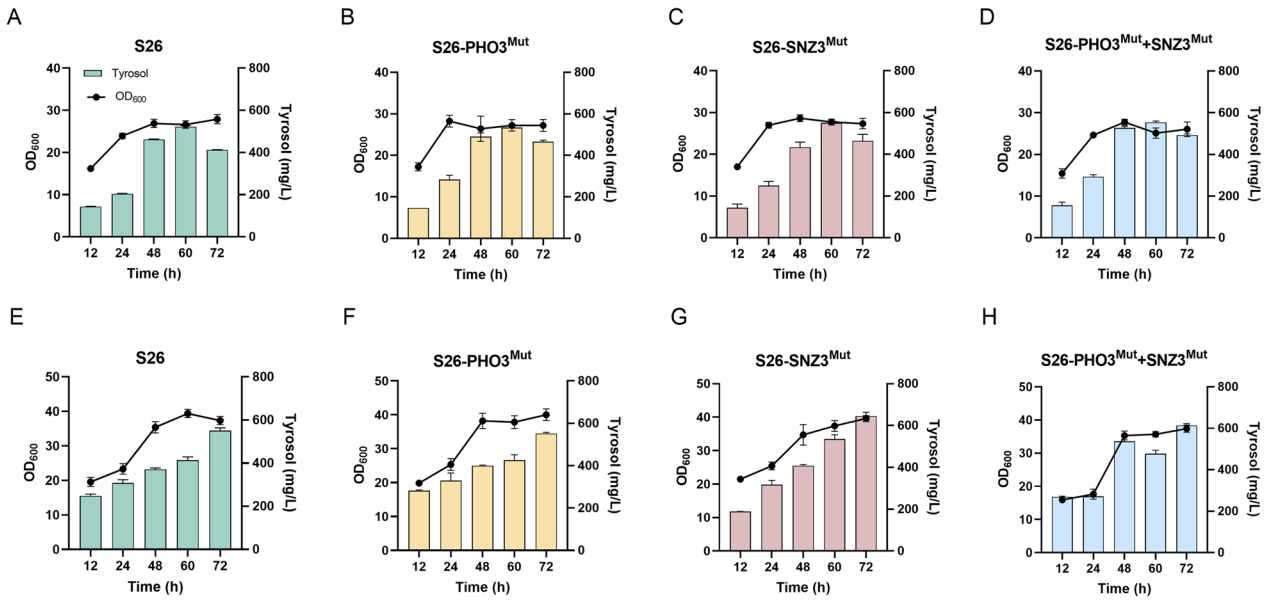

Fig. 9 **A**, **B**, **C**, and **D** The OD_{600} and tyrosol production of strains S26, S26-PHO3^{Mut}, S26-SNZ3^{Mut}, and S26-PHO3^{Mut} + SNZ3^{Mut}, which were cultured on YEPD medium supplemented with 20 g/L glucose. **E**, **F**, **G**, and **H** The OD_{600} and tyrosol production of strains S26, S26-PHO3^{Mut}, S26-SNZ3^{Mut}, and S26-PHO3^{Mut} + SNZ3^{Mut}, which were cultured on YEPD medium supplemented with 100 g/L glucose

yeast growth and help yeast produce aromatic amino acids [39, 40]. Given the function of SNZ3, we speculated that the mutation promoted the utilisation and transport of pyridoxine. The increased utilisation of pyridoxine by yeast promoted the growth of yeast in 100 g/L glucose medium. The recovery of yeast growth further promoted the production of tyrosol. Reverse engineering demonstrated that a single-nucleotide mutation in SNZ3 could increase the concentration of tyrosol.

Discussion

In this work, we performed adaptive laboratory evolution to restore the growth of the high-yield tyrosol-producing strain S26. Using glucose as a variable, we tried to balance the relationship between yeast growth and tyrosol production and then obtained a more robust industrial tyrosol-producing strain. In the evolutionary experiment, we obtained three strains after evaluating their growth and tyrosol production. We selected the S26-AE2 strain for the transcriptome analysis and genome analysis to clarify the mechanism of evolution of strain growth and tyrosol production through the above analysis.

For transcriptome analysis, we analysed the expression levels of key genes related to processes ranging from glucose metabolism to tyrosol production in yeast. The analysis of the expression of these genes revealed metabolic changes in the evolutionary strain S26-AE2, amongst which the key metabolic changes were those in the glycolysis pathway, tricarboxylic acid cycle, and tyrosol synthesis pathway. We speculate that these metabolic changes may contribute to the recovery of yeast growth and the production of tyrosol.

In the genome analysis of the evolutionary strains, we detected mutations in the key genes *PHO3* and *SNZ3*. These genes promoted yeast growth in the previous studies. *S. cerevisiae* itself can produce a certain amount of thiamine [41]. Thiamine biosynthesis is regulated by the NAD^+-dependent histone deacetylase Hst1 [42, 43]. Studies have shown that the addition of exogenous thiamine can promote ethanol production by yeast [39, 40]. In addition, regulating thiamine synthesis in *S. cerevisiae* can increase the yield of pyruvate [44]. Based on this information, we conducted reverse engineering verification to explore the effect of mutations in these genes on the growth of yeast and tyrosol production via direct mutation. Our molecular docking results revealed that mutations in these genes enhance the interaction between proteins and small molecules. After the mutations were introduced into strain S26, we determined yeast growth and found that the mutation of the *PHO3* and *SNZ3* genes was indeed beneficial for the production of the growth substrate tyrosol in yeast. However, not all mutations have beneficial effects, and studies have shown that a *PHO6* mutant of *S cerevisiae*, which lack a regulatory gene required for periplasmic thiamine synthesis and repressible acid phosphatase activity, is auxotrophic for thiamine [45, 46].

Thiamine is an essential coenzyme of phosphoketolase, which is involved in substrate activation and carbon–carbon-bond cleavage. After the combination of thiamine and phosphoketolase, a stable active complex is formed [47]. A lack of thiamine affects the activity of phosphoketolase, leading to metabolic disorders. Pyridoxine is the precursor of thiamine (Fig. 10). $PHO3^{Asn134Asp}$ and $SNZ3^{Val125Ile}$ might increase the synthesis of pyridoxine and thiamine. Adequate thiamine will theoretically help phosphoketolase increase the production of E4P, the precursor of tyrosol. Therefore, we hypothesised that the mutations of *PHO3* and *SNZ3* may be some of the reasons for the increase in tyrosol production in the S26-AE2 strain, because they alter the activity of phosphoketolase.

Conclusions

In this work, the growth of the high-yield tyrosol-producing strain S26 was restored through adaptive evolution in the laboratory. The transcriptome analysis revealed differences in gene expression between the evolutionary strain S26-AE2 and the original strain S26 in terms of glycolysis, the TCA cycle, and tyrosol synthesis pathways. Molecular docking and reverse engineering verified the effectiveness of the $SNZ3^{Val125Ile}$ mutation in increasing tyrosol production. This study provides a theoretical basis for the metabolic engineering of *S. cerevisiae* to synthesise tyrosol and its derivatives.

Materials and methods

Strain construction and cultivation

S. cerevisiae strain 26 was used in this study. YEPD medium (20 g/L peptone, 10 g/L yeast extract, and 20 g/L glucose) was used to cultivate *S. cerevisiae*, and glucose was added at a concentration of 100 g/L if needed. SC-Ura medium containing 20 g/L glucose, 6.7 g/L yeast nitrogen base (with ammonium sulphate, without ammonium acids), and 1.29 g/L Do supplement-Ura was used for yeast transformation. The yeast strains were cultured at 30 °C and shaken at 200 rpm for 72 h. *E. coli* JM110 and *E. coli* DH5α were used for the construction of plasmids and were cultured in LB medium containing 5 g/L yeast extract, 10 g/L peptone, and 10 g/L NaCl, pH 7.2. The *E. coli* were cultured at 37 °C with shaking at 200 rpm. All reagents were purchased from Shanghai Yuanye Bio-Technology Co., Ltd. (Shanghai, China). The plasmids used in this study and the primers used are listed in Table S1 and Table S2.

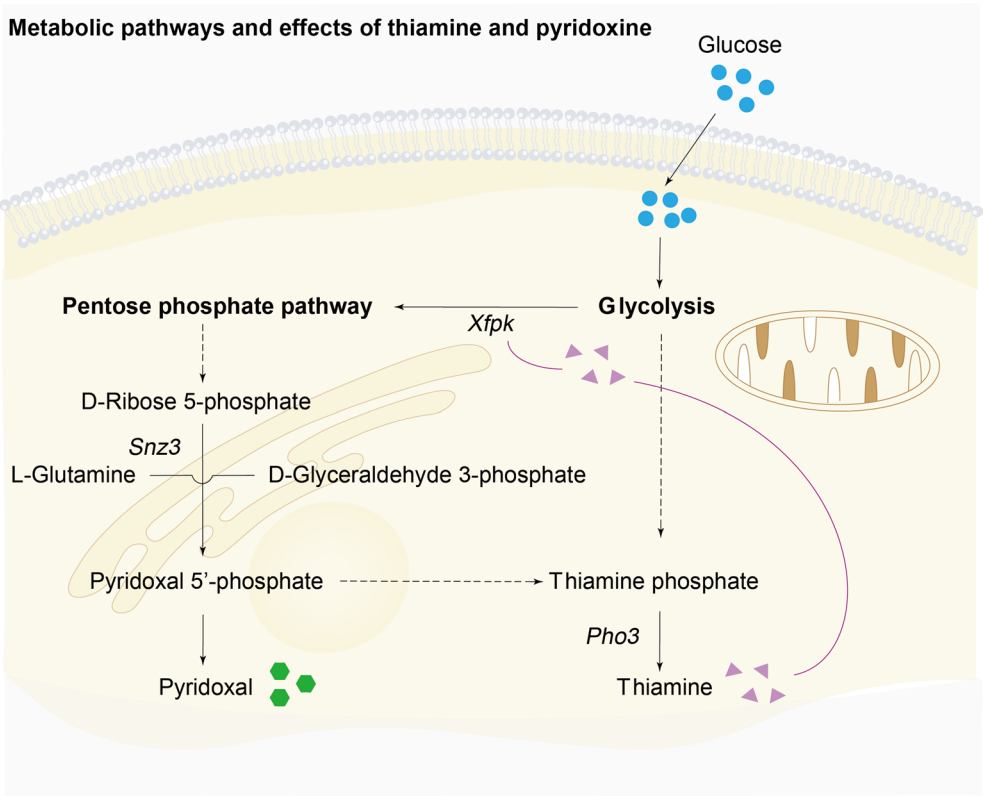

Fig. 10 Regulatory mechanism of thiamine-dependent enzymes. Xfpk is an important phosphoketolase involved in tyrosol synthesis

Adaptive laboratory evolution

S. cerevisiae S26 was used as the parental strain and cultured in a shaker flask with YEPD medium. The S26 strain suspension was seeded into EVOL cells (Luoyang Huaqing Tianmu Biotechnology Co., Ltd., Luoyang, China) [48], which enabled automatic passaging, and the OD_{600} was monitored. The initial glucose concentration of the evolution medium was 20 g/L, and the amount of added glucose gradually increased during the process of evolution. When the OD_{600} reached 15, the yeast was automatically passaged to the next generation. Samples were collected at each stage and cultured in YEPD medium with the corresponding glucose concentration. The strains were preserved in glycerol in a tube. The average passage time was calculated by dividing the total duration of each stage by the number of passages.

RNA extraction

The *S. cerevisiae* S26 and S26-AE2 strains were cultured at 30 ℃ and 200 rpm for 12 h, and the cultures were inoculated into YEPD medium or YEPD medium containing 100 g/L glucose at an initial OD_{600} of 0.5. Three biological replicates were established. The cultures were collected, and total RNA was extracted. The RNA quality was subsequently determined using a 5300 Bioanalyzer (Agilent Technologies, Santa Clara, CA, USA) and quantified using an ND-2000 (NanoDrop Technologies, Wilmington, DE, USA). Only high-quality RNA samples ($OD_{260/280}=1.8–2.2$, $OD_{260/230}\geq 2.0$, $RIN\geq 6.5$, $28S:18S\geq 1.0, >1$ μg) were used to construct the sequencing library. RNA purification, reverse transcription, library construction, and sequencing were performed at Shanghai Majorbio Biopharm Biotechnology Co., Ltd. (Shanghai, China).

Differential expression analysis

A differential expression analysis was performed using DESeq2 or DEGseq to identified differentially expressed genes (DEGs) between different samples. DEGs with $|log2FC|\geq 1$ and $FDR\leq 0.05$ (DESeq2) or $FDR\leq 0.001$ (DEGseq) were considered significantly differentially expressed genes. In addition, the DEGs were mapped to KEGG pathways, and the expression levels are presented in a heatmap.

Analytical methods

The cell density (OD_{600}) was measured with a spectrophotometer (Shanghai Jinghua Technology Instrument Co., Ltd., China). The concentrations of tyrosol and trehalose were determined by high-performance liquid chromatography (HPLC) (Thermo Fisher Scientific, Waltham, MA, USA). A Thermo-C18 column (4.6 mm × 250 mm, 5 μm) was used. The detection conditions were as follows: mobile phase containing a 0.05% (v/v) formic acid aqueous solution (A) and acetonitrile (B); gradient elution (0–20 min, 20% B; 20–25 min, 95% B; 25–35 min, 95% B; 35–40 min 95% B; 40–50 min, 10% B); column temperature of 30 ℃; flow rate of 1 mL/min; and detection wavelength of 224 nm. The trehalose content was determined using a refractive index detector with a mobile phase of 0.05 mmol/L H_2SO_4 at a flow rate of 1 mL/min and a column temperature of 50 ℃. Glucose and ethanol contents were measured using a biosensor (Sieman Technology Co., Ltd., Shenzhen, China). The glycerine determination was performed with a tissue cell triglyceride (TG) assay kit (Applygen Technologies Inc., Beijing, China). The morphology of the yeast cells was analysed with a scanning electron microscope (JEOL JSM6390LV, Tokyo, Japan).

Spot assay

S. cerevisiae was cultured in YEPD medium to the log phase of growth, and the cells were harvested by centrifugation (4000 × g, 5 min) and suspended in sterile water. Afterwards, the cells were diluted to an OD_{600} of 1 with sterile water. The yeast cells were prepared as aliquots in tenfold serial dilutions, spotted on YEPD plates and YEPD plates supplemented with 100 g/L glucose, and cultured at 30 °C for 24 h.

SNP analysis

The SNP density map was created using CMplot in the R language package (https://www.bioinformatics.com.cn/) [49]. The raw data have been uploaded to the SRA database.

Molecular docking

The structural models of the PHO3 and SNZ3 proteins were constructed with SWISS-MODEL (https://swissmodel.expasy.org/). The structures of small molecules were obtained from PubChem (https://pubchem.ncbi.nlm.nih.gov/) for docking. Molecular docking was performed using CB-Dock2 (https://cadd.labshare.cn/cb-dock2/php/index.php) [50].

DNA manipulations

The CRISPR-Cas9 system was used to modify the genome. The plasmid pML104 was used to construct gRNA expression vectors [51]. The specific guide RNA sequences were designed using the CHOPCHOP web tool (http://crispor.tefor.net) [52]. The pUC57 plasmid was first linearized with restriction enzymes, and the upstream and downstream homologous arms with mutations were ligated together using the ClonExpress MultiS One-Step Cloning Kit (Vazyme Biotech Co., Ltd., Nanjing, China) to construct homologous recombination

fragments. The gRNA expression vectors and homologous recombination fragments were cotransformed into yeast by the LiAc/ssDNA/PEG method [53]. The correct yeast clones were selected from the SC-Ura media.

Statistics and reproducibility

The significance of differences in data between groups was determined with a *t test* using GraphPad Prism 8 (GraphPad Software, San Diego, CA, USA). The data were analysed and graphed with GraphPad Prism 8. All the experiments were conducted with three biological replicates. The heatmap package in R was used to generate heatmaps and volcano plots.

Abbreviations

ACO2	Aconitate hydratase
ACS1/ACS2	Acetyl-CoA ligase
ALD6	Aldehyde dehydrogenase
ALE	Adaptive laboratory evolution
ARO10	Phenylpyruvate decarboxylase
ARO2	Bifunctional chorismate synthase/riboflavin reductase
ARO3/ARO4	3-Deoxy-7-phosphoheptulonate synthase
ARO7	Chorismate mutase
DAHP	3-Deoxy-D-arabino-heptulosonic acid 7-phosphate
DOT6	Transcriptional regulatory protein
ENO1/ENO2	Phosphopyruvate hydratase
FBA1	Fructose-bisphosphate aldolase
FBP	Fructose-1,6-bisphosphatase
GAP	Type I glyceraldehyde-3-phosphate dehydrogenase
GLK1	Glucokinase
GND1/GND2	Phosphogluconate dehydrogenase
GPD1/GPD2	Glycerol-3-phosphate dehydrogenase
GPM1/GPM2	Phosphoglycerate mutase
GPP2	Glycerol-3-phosphate dehydrogenase
GUT1	Glycerol kinase
GUT2	Glycerol-3-phosphate dehydrogenase
HXK1/HXK2	Hexokinase 1
HXT2/HXT10	High-affinity glucose transporter genes
HXT3	Low affinity glucose transporter
HXT4	Hexose transporter
HXT5	Low/medium-affinity glucose transporter
IDP2	Isocitrate dehydrogenase
LAT1	Dihydrolipoyllysine-residue acetyltransferase
LSC	Succinyl-CoA ligase
MAE1	Malate dehydrogenase
MAL32	A lpha-glucosidase
MDH2/MDH3	Malate dehydrogenase
MLS1	Malate synthase
MPC1	Mitochondrial pyruvate carrier
OA	Oxaloacetate
PDB1	Pyruvate dehydrogenase
PDC6	Indolepyruvate decarboxylase 6
PDX1	Pyridoxine biosynthesis protein 1
PEP	Phosphoenolpyruvate
PFK	Phosphofructokinase
PGI1	Phosphoglucose isomerase 1
PGK1	Phosphoglycerate kinase 1
PHK	Peterologous phosphoketolase pathway
PHO3/PHO5/PHO6	Acid phosphatase
PPP	Pentose phosphate pathway
PYC1	Pyruvate carboxylase 1
PYK1	Pyruvate kinase
RKI1	Ribose-5-phosphate isomerase
SDH	Succinate dehydrogenase membrane anchor subunit
SHH4	Succinate dehydrogenase
SNP	Single nucleotide polymorphism
SNZ3	Pyridoxal 5′-phosphate synthase
SOL3/SOL4	6-Phosphogluconolactonase
TCA	Tricarboxylic acid cycle
TKL1/TKL2	Transketolase
TYR1	Prephenate dehydrogenase ($NADP^+$)
ZWF1	$NADP^+$-dependent dehydrogenase

Supplementary Information

The online version contains supplementary material available at https://doi.org/10.1186/s13068-025-02627-4.

Supplementary material 1.

Author contributions

N S, HL X, J D, and X C designed the whole and wrote the final manuscript. XX Y, SY L, and LL X carried out the part experiments and data collection. K Z, L Y, and S H Y participated in data analysis and manuscript.

Funding

This work was supported by the National Natural Science Foundations of China (Grant Nos. 31871789 and 41876114), the key project of the Hubei Provincial Department of Education (Grant No. T2022011), and the Natural Science Foundation of Hubei Province (Grant No. 2024AFB803).

Availability of data and materials

No datasets were generated or analysed during the current study.

Declarations

Ethics approval and consent to participate

Not applicable.

Consent for publication

Not applicable.

Competing interests

The authors declare no competing interests.

Author details

[1]Cooperative Innovation Center of Industrial Fermentation (Ministry of Education & Hubei Province), Key Laboratory of Fermentation Engineering (Ministry of Education), National "111" Center for Cellular Regulation and Molecular Pharmaceutics, Hubei Key Laboratory of Industrial Microbiology, School of Life and Health Sciences, Hubei University of Technology, No. 28, Nanli Road, Hongshan District, Wuhan 430068, Hubei, People's Republic of China. [2]College of Biological and Food Engineering, Huanghuai University, Zhumadian 463000, People's Republic of China. [3]School of Food Science and Engineering, Wuhan Polytechnic University, Wuhan 430023, People's Republic of China. [4]State Key Laboratory of Biocatalysis and Enzyme Engineering, School of Life Sciences, Hubei University, Wuhan 430062, Hubei, People's Republic of China.

Received: 18 December 2024 Accepted: 15 February 2025
Published online: 05 March 2025

References

1. Kim YY, Lee S, Kim MJ, Kang BC, Dhakal H, Choi YA, et al. Tyrosol attenuates lipopolysaccharide-induced acute lung injury by inhibiting the inflammatory response and maintaining the alveolar capillary barrier. Food Chem Toxicol. 2017;1091:526–33.
2. St-Laurent-Thibault C, Arseneault M, Longpré F, Ramassamy C. Tyrosol and hydroxytyrosol, two main components of olive oil, protect N2a cells against amyloid-β-induced toxicity. Involvement of the NF-κB signaling. Curr Alzheimer Res. 2011;85:543–51.

3. Cardinali A, Pati S, Minervini F, D'Antuono I, Linsalata V, Lattanzio V. Verbascoside, isoverbascoside, and their derivatives recovered from olive mill wastewater as possible food antioxidants. J Agric Food Chem. 2012;607:1822–9.
4. Dewapriya P, Li YX, Himaya SWA, Kim SK. Isolation and characterization of marine-derived Mucor sp. for the fermentative production of tyrosol. Process Biochem. 2014;499:1402–8.
5. Begines P, Biedermann D, Valentová K, Petrásková L, Pelantová H, Maya I, et al. Chemoenzymatic synthesis and radical scavenging of sulfated hydroxytyrosol, tyrosol, and acetylated derivatives. J Agric Food Chem. 2019;6726:7281–8.
6. Flourat AL, Combes J, Bailly-Maitre-Grand C, Magnien K, Haudrechy A, Renault JH, et al. Accessing *p*-hydroxycinnamic acids: chemical synthesis, biomass recovery, or engineered microbial production? Chem Sus Chem. 2021;141:118–29.
7. Chung D, Kim SY, Ahn JH. Production of three phenylethanoids, tyrosol, hydroxytyrosol, and salidroside, using plant genes expressing in *Escherichia coli*. Sci Rep. 2017;71:2578.
8. Guo W, Huang Q, Feng Y, Tan T, Niu S, Hou S, et al. Rewiring central carbon metabolism for tyrosol and salidroside production in *Saccharomyces cerevisiae*. Biotechnol Bioeng. 2020;1178:2410–9.
9. Yang H, Xue Y, Yang C, Shen W, Fan Y, Chen X. Modular engineering of tyrosol production in *Escherichia coli*. J Agric Food Chem. 2019;6714:3900–8.
10. Liu H, Tian Y, Zhou Y, Kan Y, Wu T, Xiao W, et al. Multi-modular engineering of *Saccharomyces cerevisiae* for high-titre production of tyrosol and salidroside. Microb Biotechnol. 2021;146:2605–16.
11. Liu H, Xiao Q, Wu X, Ma H, Li J, Guo X, et al. Mechanistic investigation of a D to N mutation in DAHP synthase that dictates carbon flux into the shikimate pathway in yeast. Commun Chem. 2023;61:152.
12. Jiaojiao YSZ, Jingwen Z. Metabolic engineering of *Escherichia coli* for improving tyrosol production. Food Ferment Ind. 2021;4722:8–15.
13. Dragosits M, Mattanovich D. Adaptive laboratory evolution – principles and applications for biotechnology. Microb Cell Fact. 2013;12:64.
14. Sandberg TE, Salazar MJ, Weng LL, Palsson BO, Feist AM. The emergence of adaptive laboratory evolution as an efficient tool for biological discovery and industrial biotechnology. Metab Eng. 2019;56:1–16.
15. Dai Z, Huang M, Chen Y, Siewers V, Nielsen J. Global rewiring of cellular metabolism renders *Saccharomyces cerevisiae* Crabtree negative. Nat Commun. 2018;91:3059.
16. Ingelman H, Heffernan JK, Harris A, Brown SD, Shaikh KM, Saqib AY, et al. Autotrophic adaptive laboratory evolution of the acetogen *Clostridium autoethanogenum* delivers the gas-fermenting strain *LAbrini* with superior growth, products, and robustness. N Biotechnol. 2024;83:1–15.
17. Hong KK, Vongsangnak W, Vemuri GN, Nielsen J. Unravelling evolutionary strategies of yeast for improving galactose utilization through integrated systems level analysis. Proc Natl Acad Sci U S A. 2011;10829:12179–84.
18. LaCroix RA, Sandberg TE, O'Brien EJ, Utrilla J, Ebrahim A, Guzman GI, et al. Use of adaptive laboratory evolution to discover key mutations enabling rapid growth of *Escherichia coli* K-12 MG1655 on glucose minimal medium. Appl Environ Microbiol. 2015;811:17–30.
19. Pfeifer E, Gätgens C, Polen T, Frunzke J. Adaptive laboratory evolution of *Corynebacterium glutamicum* towards higher growth rates on glucose minimal medium. Sci Rep. 2017;71:16780.
20. Song N, Xia H, Xie Y, Guo S, Zhou R, Shangguan L, et al. Semi-rational design and modification of phosphoketolase to improve the yield of tyrosol in *Saccharomyces cerevisiae*. Synth Syst Biotechnol. 2025;101:294–306.
21. Buziol S, Becker J, Baumeister A, Jung S, Mauch K, Reuss M, et al. Determination of in vivo kinetics of the starvation-induced Hxt5 glucose transporter of *Saccharomyces cerevisiae*. FEMS Yeast Res. 2002;23:283–91.
22. Herrero P, Flores L, de la Cera T, Moreno F. Functional characterization of transcriptional regulatory elements in the upstream region of the yeast GLK1 gene. Biochem J. 1999;343(2):319–25.
23. Rodríguez A, De La Cera T, Herrero P, Moreno F. The hexokinase 2 protein regulates the expression of the GLK1, HXK1 and HXK2 genes of *Saccharomyces cerevisiae*. Biochem J. 2001;355:625–31.
24. Müller H, Lesur A, Dittmar G, Gentzel M, Kettner K. Proteomic consequences of TDA1 deficiency in *Saccharomyces cerevisiae*: protein kinase Tda1 is essential for Hxk1 and Hxk2 serine 15 phosphorylation. Sci Rep. 2022;121:18084.
25. Jin C, Kim S, Moon S, Jin H, Hahn JS. Efficient production of shinorine, a natural sunscreen material, from glucose and xylose by deleting HXK2 encoding hexokinase in *Saccharomyces cerevisiae*. FEMS Yeast Res. 2021. https://doi.org/10.1093/femsyr/foab053.
26. Lane S, Xu H, Oh EJ, Kim H, Lesmana A, Jeong D, et al. Glucose repression can be alleviated by reducing glucose phosphorylation rate in *Saccharomyces cerevisiae*. Sci Rep. 2018;81:2613.
27. Moreno F, Herrero P. The hexokinase 2-dependent glucose signal transduction pathway of *Saccharomyces cerevisiae*. FEMS Microbiol Rev. 2002;261:83–90.
28. Heux S, Cadiere A, Dequin S. Glucose utilization of strains lacking PGI1 and expressing a transhydrogenase suggests differences in the pentose phosphate capacity among *Saccharomyces cerevisiae* strains. FEMS Yeast Res. 2008;82:217–24.
29. Rep M, Albertyn J, Thevelein JM, Prior BA, Hohmann S. Different signalling pathways contribute to the control of GPD1 gene expression by osmotic stress in *Saccharomyces cerevisiae*. Microbiology (Reading). 1999;1453:715–27.
30. Jagtap RS, Mahajan DM, Mistry SR, Bilaiya M, Singh RK, Jain R. Improving ethanol yields in sugarcane molasses fermentation by engineering the high osmolarity glycerol pathway while maintaining osmotolerance in *Saccharomyces cerevisiae*. Appl Microbiol Biotechnol. 2019;1032:1031–42.
31. Awasthy C, Hefny ZA, Van Genechten W, Himmelreich U, Van Dijck P. Involvement of 2-deoxyglucose-6-phosphate phosphatases in facilitating resilience against ionic and osmotic stress in *Saccharomyces cerevisiae*. Microbiol Spectr. 2024;128:13624.
32. Grauslund M, Rønnow B. Carbon source-dependent transcriptional regulation of the mitochondrial glycerol-3-phosphate dehydrogenase gene, GUT2, from *Saccharomyces cerevisiae*. Can J Microbiol. 2000;4612:1096–100.
33. Boles E, de Jong-Gubbels P, Pronk JT. Identification and characterization of MAE1, the *Saccharomyces cerevisiae* structural gene encoding mitochondrial malic enzyme. J Bacteriol. 1998;18011:2875–82.
34. Bergman A, Hellgren J, Moritz T, Siewers V, Nielsen J, Chen Y. Heterologous phosphoketolase expression redirects flux towards acetate, perturbs sugar phosphate pools and increases respiratory demand in *Saccharomyces cerevisiae*. Microb Cell Fact. 2019;181:25.
35. Regmi P, Knesebeck M, Boles E, Weuster-Botz D, Oreb M. A comparative analysis of NADPH supply strategies in *Saccharomyces cerevisiae*: Production of d-xylitol from d-xylose as a case study. Metab Eng Commun. 2024;19:245.
36. Rendulić T, Perpelea A, Ortiz JPR, Casal M, Nevoigt E. Mitochondrial membrane transporters as attractive targets for the fermentative production of succinic acid from glycerol in *Saccharomyces cerevisiae*. FEMS Yeast Res. 2024. https://doi.org/10.1093/femsyr/foae009.
37. Marques WL, Mans R, Marella ER, Cordeiro RL, van den Broek M, Daran JG, et al. Elimination of sucrose transport and hydrolysis in *Saccharomyces cerevisiae*: a platform strain for engineering sucrose metabolism. FEMS Yeast Res. 2017. https://doi.org/10.1093/femsyr/fox006.
38. Paxhia MD, Downs DM. SNZ3 encodes a PLP synthase involved in thiamine synthesis in *Saccharomyces cerevisiae*. G3. 2019;92:335–44.
39. Evers MS, Roullier-Gall C, Morge C, Sparrow C, Gobert A, Vichi S, et al. Thiamine and biotin: relevance in the production of volatile and non-volatile compounds during *Saccharomyces cerevisiae* alcoholic fermentation in synthetic grape must. Foods. 2023;125:972.
40. Labuschagne P, Divol B. Thiamine: a key nutrient for yeasts during wine alcoholic fermentation. Appl Microbiol Biotechnol. 2021;1053:953–73.
41. Rocchi R, Wolkers-Rooijackers JCM, Liao Z, Tempelaars MH, Smid EJ. Strain diversity in *Saccharomyces cerevisiae* thiamine production capacity. Yeast. 2023;4012:628–39.
42. Li M, Petteys BJ, McClure JM, Valsakumar V, Bekiranov S, Frank EL, et al. Thiamine biosynthesis in *Saccharomyces cerevisiae* is regulated by the NAD+-dependent histone deacetylase Hst1. Mol Cell Biol. 2010;3013:3329–41.
43. Labuschagne PWJ, Rollero S, Divol B. Comparative uptake of exogenous thiamine and subsequent metabolic footprint in *Saccharomyces cerevisiae* and *Kluyveromyces marxianus* under simulated oenological conditions. Int J Food Microbiol. 2021;354:109206.

44. Xu G, Hua Q, Duan N, Liu L, Chen J. Regulation of thiamine synthesis in *Saccharomyces cerevisiae* for improved pyruvate production. Yeast. 2012;296:209–17.
45. Kawasaki Y, Nosaka K, Kaneko Y, Nishimura H, Iwashima A. Regulation of thiamine biosynthesis in *Saccharomyces cerevisiae*. J Bacteriol. 1990;17210:6145–7.
46. Ehrmann AK, Wronska AK, Perli T, de Hulster EAF, Luttik MAH, van den Broek M, et al. Engineering *Saccharomyces cerevisiae* for fast vitamin-independent aerobic growth. Metab Eng. 2024;82:201–15.
47. Libuda F, Phosphoketolase - A mechanistic update, in: Department of Molecular Structural Biology, University Göttingen, 2018; 141.
48. Li L, Zhang Q, Shi R, Yao M, Tian K, Lu F, et al. Multidimensional combinatorial screening for high-level production of erythritol in *Yarrowia lipolytica*. Bioresour Technol. 2024;406:131035.
49. Tang D, Chen M, Huang X, Zhang G, Zeng L, Zhang G, et al. SRplot: a free online platform for data visualization and graphing. PLoS ONE. 2023;1811:e0294236.
50. Liu Y, Yang X, Gan J, Chen S, Xiao ZX, Cao Y. CB-Dock2: improved protein-ligand blind docking by integrating cavity detection, docking and homologous template fitting. Nucleic Acids Res. 2022;501:159–64.
51. Laughery MF, Wyrick JJ. Simple CRISPR-Cas9 Genome Editing in *Saccharomyces cerevisiae*. Curr Protoc Mol Biol. 2019;1291:110.
52. Labun K, Montague TG, Gagnon JA, Thyme SB, Valen E. CHOPCHOP v2: a web tool for the next generation of CRISPR genome engineering. Nucleic Acids Res. 2016;441:272–6.
53. Gietz RD, Schiestl RH. High-efficiency yeast transformation using the LiAc/SS carrier DNA/PEG method. Nat Protoc. 2007;21:31–4.

Publisher's Note